MIGRAINE AND PATHOPHYSIOLOGY

KEY NOTE LECTURE

K. Michael A. Welch
Vijaya Nagesh
Sheena K. Aurora
Neil Gelman

Periaqueductal gray matter dysfunction in migraine and chronic daily headache may be due to free radical damage

K.M.A. Welch (✉)
University of Kansas Medical Center,
3901 Rainbow Blvd.,
Room 6002 Wescoe,
Kansas City, Kansas 66160-7702, USA
e-mail: kwelch2@kumc.edu
Tel.: +1-913-588-5448
Fax: +1-913-588-5444

V. Nagesh • S.K. Aurora • N. Gelman
Department of Neurology,
Henry Ford Health Sciences Center
and NMR Research Center,
Detroit, Michigan, USA

Abstract The periaqueductal gray matter (PAG) is at the center of a powerful descending antinociceptive neuronal network. We studied iron homeostasis in the PAG in episodic migraine patients between attacks and in chronic daily headache patients during headache using high-resolution magnetic resonance imaging (MRI) techniques to map the transverse relaxation rates R2, R2* and R2' in the PAG, red nucleus (RN) and substantia nigra (SN). R2' is a measure of non-heme iron in tissues. We hypothesized that repeated hyperoxia of brainstem structures observed during migraine may generate free radical damage over time, resulting in iron deposition in vulnerable tissue. Seventeen patients diagnosed with episodic migraine with and without aura (EM), 17 with chronic daily headache (CDH) and medication overuse, and 17 normal adults (N) were imaged with a 3 tesla MRI system. In the PAG, there was a significant increase in mean R2' and R2* values in both the EM and CDH groups ($p<0.05$) compared to normal, but no significant difference in these values between the EM and CDH groups, or between migraine with or without aura in the EM group. Positive correlations were found for duration of illness with R2' in the EM and CDH groups. Duration of the episodic migraine stage in the CDH group did not correlate significantly with R2', although the total duration of the episodic migraine plus daily headache stages of the CDH group strongly correlated with R2'. No effect of age was noted on R2'. Decrease in mean R2' and R2* values also was observed in the RN and SN of the CDH compared to N and EM groups ($p<0.05$), explained best by flow activation due to head pain. Iron homeostasis in the PAG was selectively, persistently and progressively impaired in the EM and CDH groups, possibly caused by free radicals generated during repeated migraine attacks. These results support and emphasize the role of the PAG in migraine, potentially by dysfunctional control of the trigeminovascular nociceptive system. Development of CDH out of EM may be associated with a critical threshold of iron deposition and drug withdrawal excitation of the dysfunctional PAG.

Introduction

The periaqueductal gray matter (PAG) is the center of a powerful descending antinociceptive neuronal network [1]. The concentration of transferrin receptors that transport iron in and out of the PAG is the highest of any brain region [2]; transferrin receptor density may be a marker of the cellular requirements for iron during oxidative metabolism [3]. Those neurons that have high resting iron levels and the potential for iron-induced oxidative stress may be selectively vulnerable to free radical damage [4]. We have observed previously that hyperoxia occurs in brainstem structures activated during migraine attacks. Overexpression of transferrin receptors may lead to tissue iron accumulation and iron-catalyzed free radical cell damage, accentuated by repeated episodes of hyperoxia recorded during migraine with or without aura [5, 6]. We report here increased R2' values, a sensitive MRI measure of free iron in brain tissue [7], in the PAG of patients with episodic migraine with and without aura and with chronic daily headache. These data may reflect impaired iron homeostasis, possibly associated with neuronal dysfunction or damage.

Patients and methods

Patients

International Headache Society (IHS) classification guidelines were used to diagnose episodic migraine without aura (MwoA), migraine with aura (MwA), and chronic daily headache (CDH) (>15 headaches/month) due to medication overuse in patients who had previously suffered episodic migraine without aura [8]. The Institutional Review Board of Henry Ford Health Sciences Center approved the imaging protocol. All subjects who participated in the study provided written informed consent prior to the study.

The first group consisted of 17 patients with episodic migraine (EM), including 9 MwoA patients and 8 MwA patients; 2 men and 15 women aged 23–52 years (mean age±SD, 33±10 years) were imaged. No migraine attack had occurred and no medication was taken, either abortive or preventive, within one week of study. The second group was composed of 17 patients with chronic daily headache (CDH) preceded by episodic migraine without aura attacks; 3 men and 14 women aged 21–57 years (mean age±SD, 36±10 years) were imaged. Patients were taking pain medications that included codeine and butalbital, as well as miscellaneous migraine-preventive drugs. All patients were experiencing headache at the time of imaging. The third group studied consisted of 17 healthy normal adults (N), 7 men and 10 women aged 20–64 years (mean age±SD, 38±12 years). The difference in the mean age of the three groups was not statistically significant (p=0.89, repeated measure ANOVA). The duration of illness was recorded for the EM group and the duration of CDH, including previous years of episodic migraine, was also recorded.

Techniques

All MR images were acquired with a 3 tesla, 80-cm (inner diameter) magnet (Magnex Scientific, Abingdon, England) with a maximum gradient strength of 18 mT/m and 250 μs ramp time. A quadrature birdcage head coil was used for imaging.

Multi-slice measurements of R2, R2' and R2* were performed in a single acquisition using the gradient-echo sampling of free induction decay and echo (GESFIDE) sequence [9]. The timing of the echoes in this sequence was identical to that used previously [7]. A 128x128 imaging matrix with a 220-mm field of view, and 2500 ms repetition time were used for image acquisition. The imaging time of the entire protocol, inclusive of positioning and shimming, was approximately 20 min.

Image analysis

The image sets were Fourier transformed and zero-filled to yield 256x256 in-plane images for each of the 176 two-dimensional images (16 slices x 11 echoes). Maps of R2, R2' and R2* were obtained as described in a previous study [7]. Brain tissue segmentation was performed using the iterative self-organizing data analysis technique (ISODATA) [10].

For each subject, all image slices reconstructed from the final echo (TE/TR=98/2500 ms) of the GESFIDE sequence were reviewed visually to identify and localize slices containing the PAG, red nucleus (RN), and substantia nigra (SN). The PAG, RN and SN were visible in two or more slices for all cases reported in this study. ISODATA segmentation was used to accurately delineate and identify the entire volume of the PAG, RN and SN. For each subject, the R2 (1/T2), R2* (1/ T2*) and R2' (1/T2*-1/T2) relaxation rates of the RN, SN and PAG were obtained for the left and right sides separately by projecting the corresponding segmented zones onto the maps. Measurements derived from multiple slices for each subject were expressed as a weighted average.

Statistical analysis

The relaxation rates, R2, R2' and R2* of PAG, RN, and SN for each subject are presented as mean (SD). One-way analysis of variance (ANOVA) was used to test the null hypothesis of equality of population means among the three groups; Student's paired t test was used to compare the relaxation rates for the right versus left sides. In addition, t tests were performed intra-group to compare differences in relaxation rates between the genders. Correlation analysis also was performed intra-group to determine the relationship between variables, and Pearson's product moment correlation coefficient was calculated to determine the extent of linear relationship. Significance levels were set at $p<0.05$.

Results

Representative images containing the PAG, RN or SN of a subject are shown in Fig. 1. ISODATA segmentation and classification of the different zones are illustrated in Fig. 2. Representative maps of R2, R2' and R2* for a section through the midbrain are shown in Fig. 3.

The R2, R2' and R2* values obtained for the PAG, RN, and SN for the N, EM and CDH groups are presented in Table 1. Using Student's paired t test, no intra-group side-to-side differences (left-to-right hemispheres) were noted in the relaxation rates of the PAG, RN, and SN of any of the groups. Therefore, results from both sides were pooled. Also, there were no gender-related differences in the relaxation rates of these structures for all three groups. The mean R2 values among the three groups in the PAG, RN and SN were not significantly different. Similar results were observed for both the left and right sides.

In the PAG there was a statistically significant increase in R2' and R2* values in both the EM and CDH groups ($p<0.05$) compared to the normal group (Table 1). No statistically significant differences were noted between the MwoA and MwA patients so that the results were pooled as the EM group. There was no significant difference in either the R2' value or the R2* values between the EM and CDH groups. For the N, EM and CDH groups, we performed correlation analysis of the age of the subject with the R2' value; no association was observed for either group nor for the groups combined (Fig. 4). A positive correlation was noted between the duration of illness and the increase in R2' for the EM group and for the daily headache stage in the CDH group, but no significant difference between the slopes (Fig. 5). Duration of the episodic migraine stage in the CDH group did not correlate significantly with R2' (Fig. 6), although the total duration of the episodic migraine plus daily headache stages of the CDH group strongly correlated with R2' (Fig. 7).

The intercepts of the slopes in Fig. 5 were nearly identical, 5.57, 5.67. This, plus the higher mean R2' values in both headache groups compared to control, may suggest that R2' values were high at the outset or earliest stages of illness.

No differences in R2' and R2* were observed in the RN and SN of the EM patients (Table 1). A significant decrease in R2' and R2* values of the RN and SN was found in the CDH patients compared to N and EM groups ($p<0.05$), but there was no significant difference in the relaxation rates of either the SN or RN between the N and EM groups.
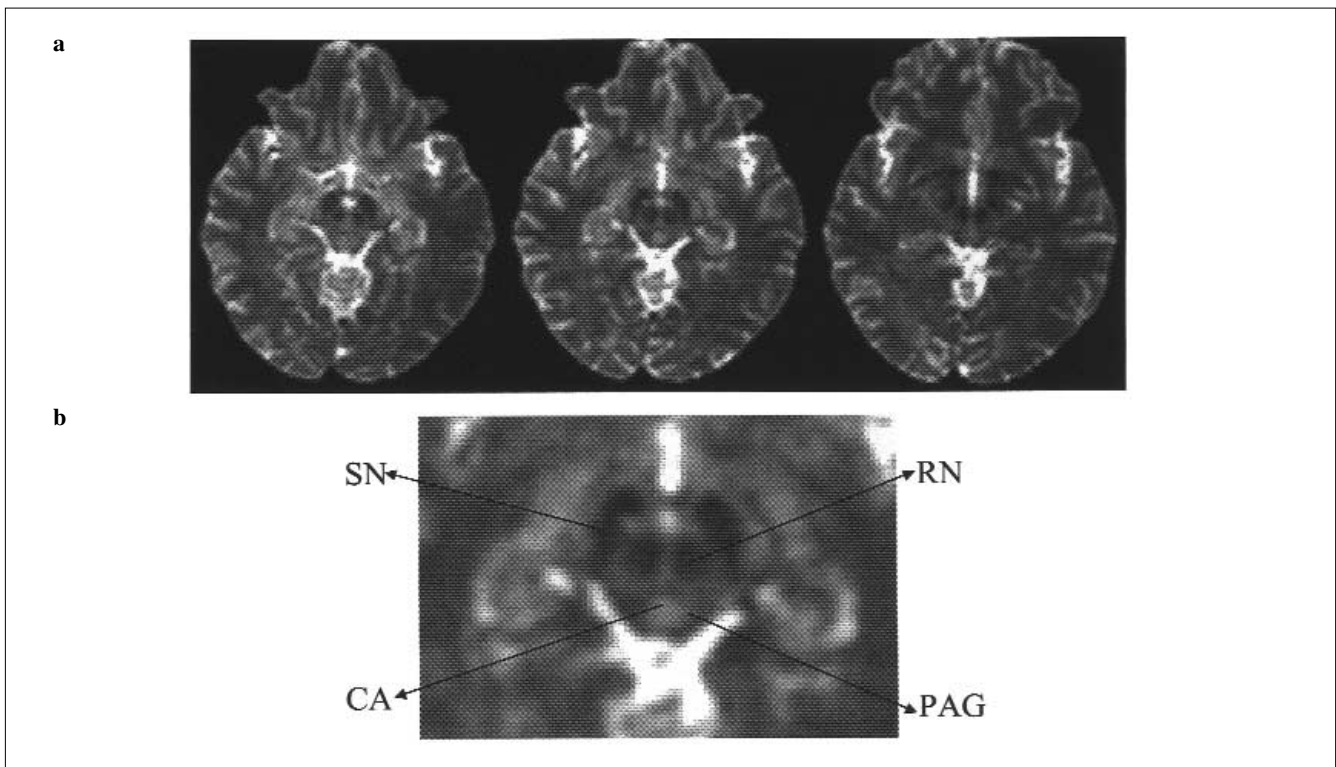

Fig. 1a, b *Representative images of PAG, RN and SN of one subject.* **a** Spin-echo MR images (echo time/repetition time (TE/TR), 98/2500 ms) of three contiguous 2.2-mm slices obtained with the gradient-echo sampling of free induction decay and echo (GESFIDE) sequence. **b** Magnified view of the center image of **a**. The hypointense areas correspond to the substantia nigra (*SN*) and the red nucleus (*RN*). The hyperintense area (*CA*) is the cerebral aqueduct, and surrounding CA is the periaqueductal gray matter (*PAG*)
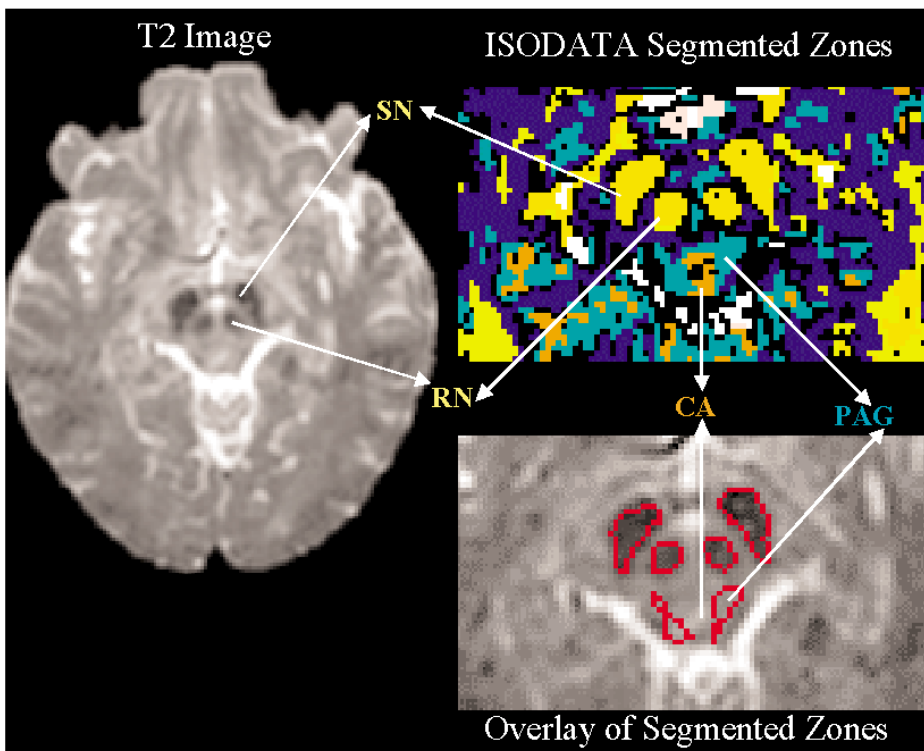
Fig. 2 Results of ISODATA segmentation and the segmented zones superimposed on the T2 image (*enlarged view*) are displayed in the *top* and *bottom panels*, respectively, on the *right*. The T2-weighted spin echo image (TE/TR, 98/2500 ms) in the *left panel* shows a region of the midbrain containing the cerebral aqueduct (*CA*), periaqueductal gray matter (*PAG*), red nucleus (*RN*) and substantia nigra (*SN*). Eleven images, one from each echo of the GESFIDE pulse sequence, were used in the computer cluster analysis (ISODATA) to segment brain tissue. Each color of the ISODATA segmented image represents a different cluster with unique properties in feature space

Fig. 3a, b *Representative maps of R2, R2' and R2* for a section through the midbrain.* **a** Maps of the transverse relaxation rates R2, R2' and R2* from a single 2.2-mm slice. Image reconstruction and calculation for these maps are detailed in the text. **b** Enlarged views of the corresponding map detailing the brainstem structures that were studied. The red nucleus (*RN*) and substantia nigra (*SN*) appear hyperintense on the three relaxation rate maps. The iso-intense area surrounding the cerebral aqueduct (*CA*) is the periaqueductal gray matter (*PAG*)
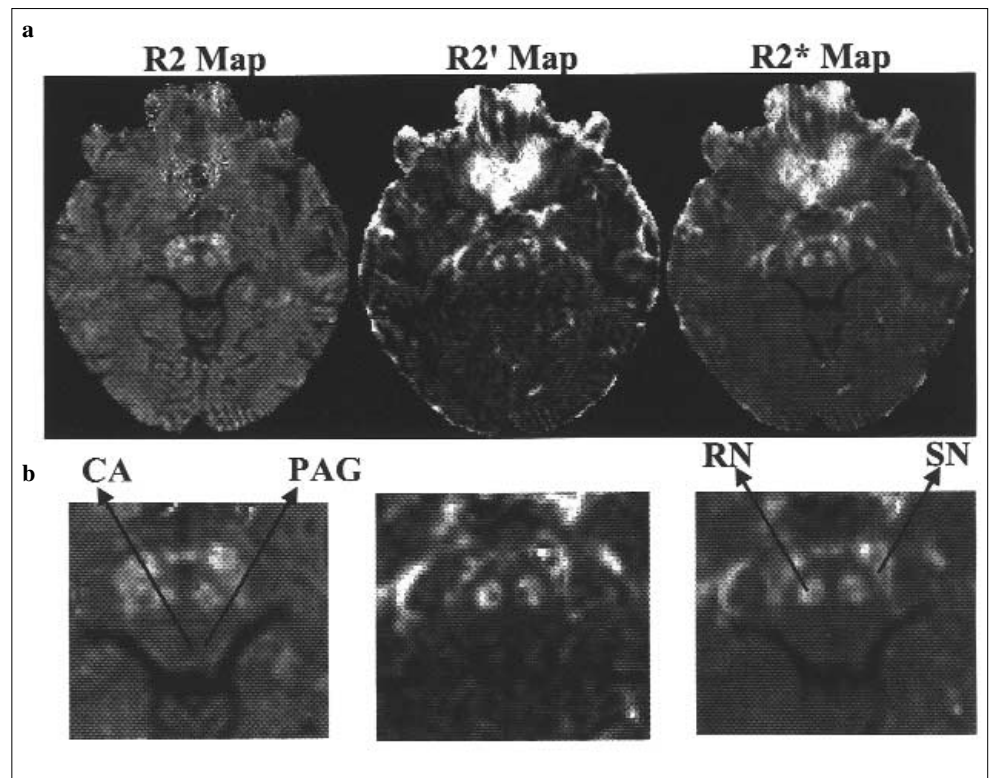
Table 1 Transverse relaxation rates R2', R2* and R2 in the periaqueductal gray matter, red nucleus and substantia nigra of normal adults and patients with episodic migraine or chronic daily headache. Values are means (SD)

Parameter	Control (n=17)	Episodic migraine (n=17)	Chronic daily headache (n=17)
Periaqueductal gray matter			
R2'	4.33 (0.97)	6.11 (0.88) #	6.36 (1.29) #
R2*	21.11 (1.25)	23.07 (1.53) #	23.58 (1.90) #
R2	17.01 (1.11)	17.10 (1.18)	17.20 (1.65)
Red nucleus			
R2'	14.30 (2.18)	13.80 (1.86)	10.70 (2.33) †
R2*	39.10 (2.85)	39.10 (3.07)	34.20 (3.02) †
R2	24.07 (1.62)	25.20 (1.98)	23.60 (1.45)
Substantia nigra			
R2'	15.10 (2.20)	15.00 (1.94)	11.60 (2.96) †
R2*	42.50 (3.01)	42.20 (3.27)	36.50 (3.35) †
R2	24.07 (1.62)	25.20 (1.98)	23.60 (1.45)

\# Significantly elevated ($p<0.05$) compared to control group
† Significantly reduced ($p<0.05$) compared to control group
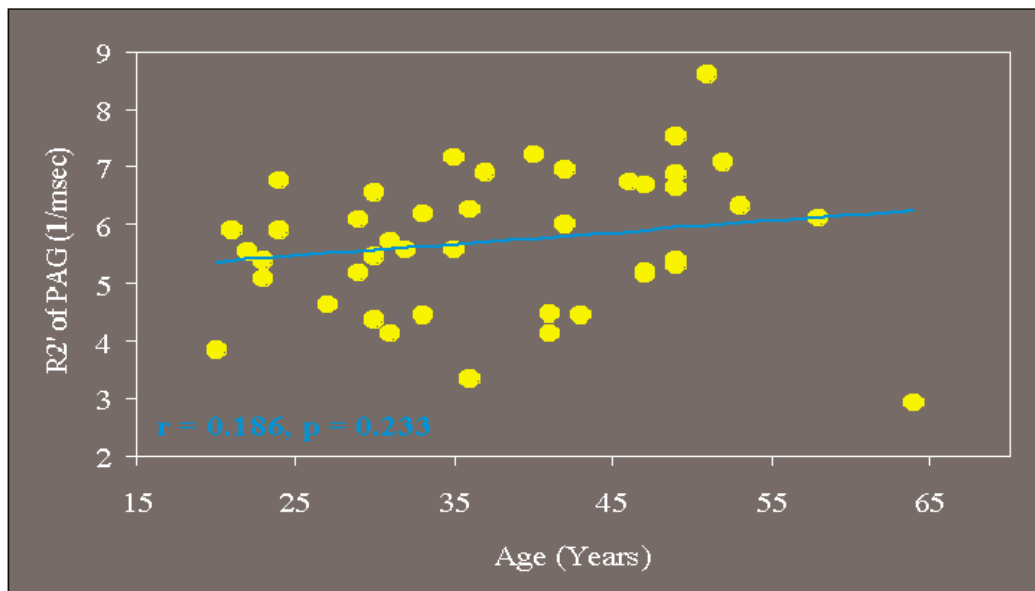
Fig. 4 Correlation analysis of age (for combined control and migraine subjects) with R2' value. The slope of the regression line is not significant
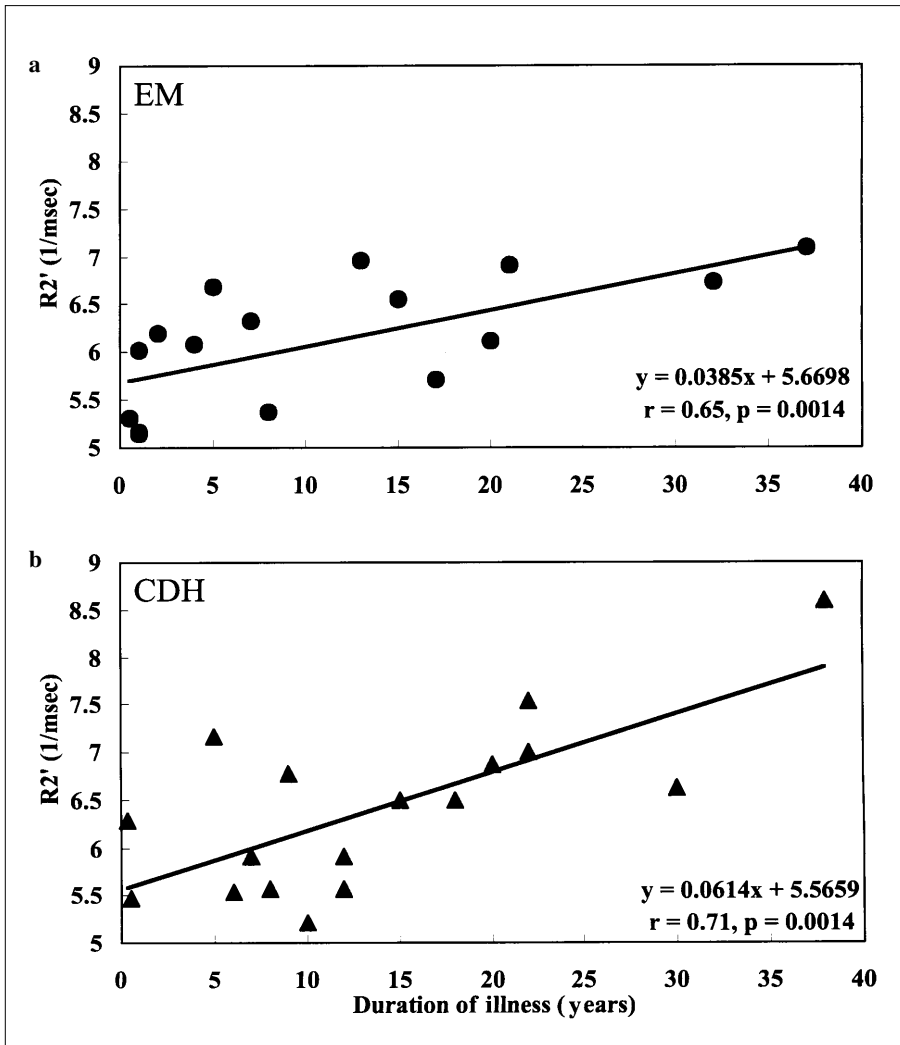
Fig. 5a, b *Correlation analysis of the duration of illness with R2' value.* **a** EM group. Correlation coefficient, r=0.65 (*p*=0.0052). **b** CDH group. r=0.71 (*p*=0.0053). Intercepts of the regression line are 5.6698 ms^{-1} for EM and 5.5659 ms^{-1} for CDH. There is no significant difference between the slopes of the regression lines of the EM and CDH groups

Fig. 6 Correlation analysis of the duration of the episodic phase (EM) of attacks in CDH patients with the R2' value. The slope of the regression line is not significant
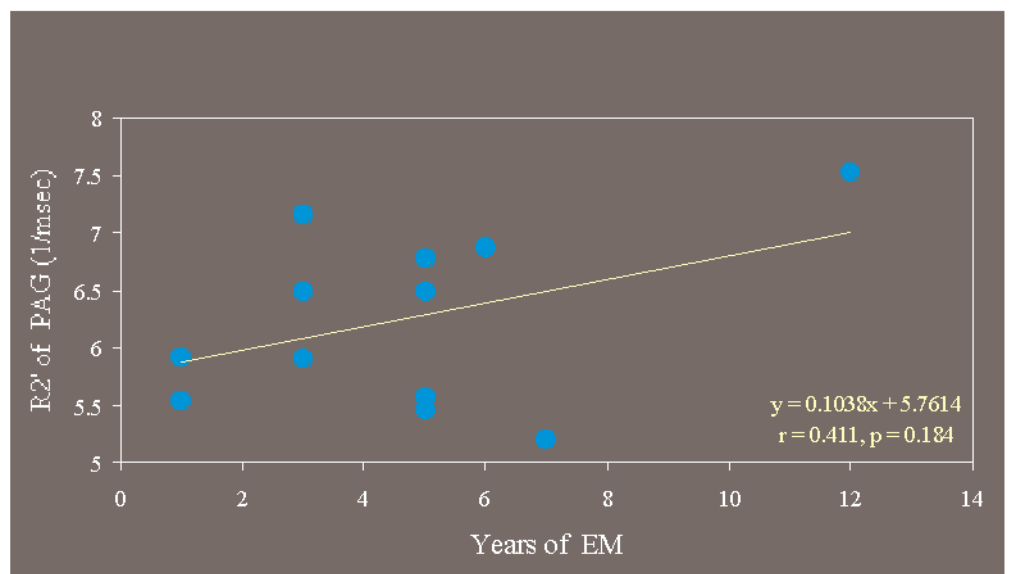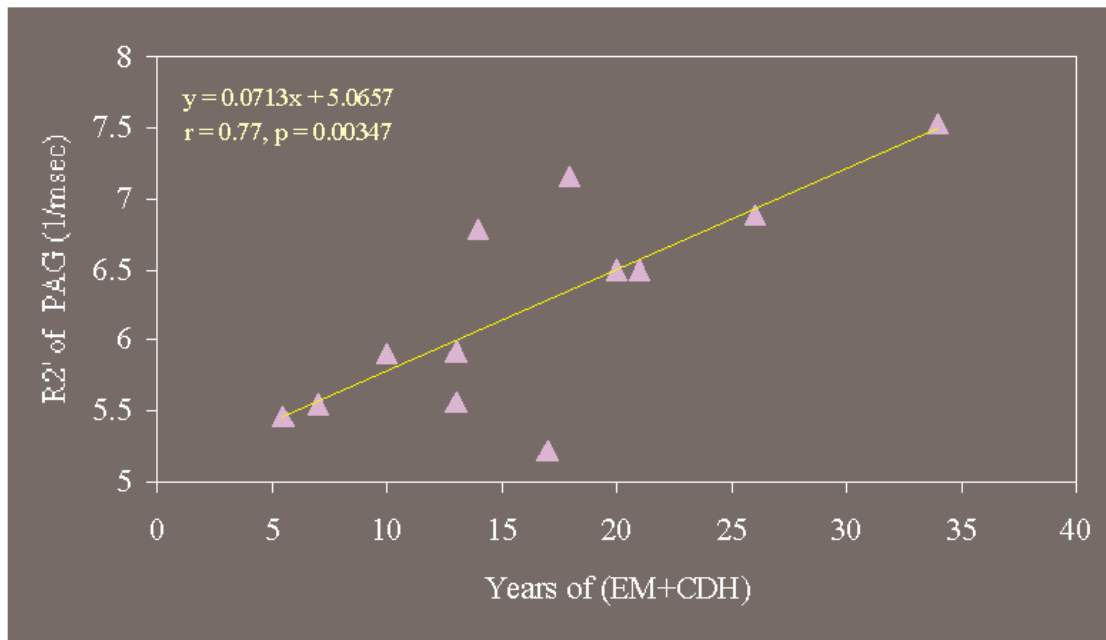
Fig. 7 Correlation analysis of the duration of the episodic and chronic headache phases of the CDH group with the R2' value. Unlike for the episodic phase (Fig. 6), there is now a significant slope of the regression line

Discussion

Raskin, Hosobuchi and Lamb first drew attention to the potential for PAG dysfunction in migraine, observing that patients with PAG electrode implantation for chronic pain sometimes developed headache resembling migraine [11]. A discrete sclerotic lesion in the PAG caused severe headache in a single case report [12]. In positron emission tomography (PET) studies during spontaneous migraine without aura, increased blood flow was measured in mesencephalic regions that possibly reflected PAG, dorsal raphe nuclei (DRN), and locus ceruleus (LC) activation, raising consideration of a brainstem "generator" of migraine attacks [13].

The midbrain PAG is an anatomically heterogeneous, functionally diverse region of densely layered neurons surrounding the aqueduct of Sylvius [14]. Receiving input from the frontal cortex and hypothalamus, and projecting to the rostral ventromedial medulla thence to the medullary and spinal dorsal horn, the PAG is the center of a powerful antinociceptive network. Furthermore, the PAG can be considered a major nodal point in the central nervous system (CNS), regulating autonomic adjustments to antinociceptive and behavioral responses to threat [15].

These observations prompted study of iron homeostasis in the PAG of migraine patients; elevation or decline in tissue iron is associated with altered cellular function [2]. Using high-resolution MRI techniques, we have mapped transverse relaxation rates R2, R2' and R2* in episodic migraine (EM) patients and in patients with chronic daily headache (CDH) and compared them to normal controls. Increase in R2' is specific to deposition of non-heme iron in tissues [7]. Decrease in R2' and R2* reflects the influence of free iron from deoxyhemoglobin [5, 6].

Iron levels were equally elevated in the PAG of migraine with or without aura. Not only was a significant increase in tissue non-heme iron found in both episodic migraine and the daily headache groups compared to controls, but levels increased with the duration of illness. Because there was no influence of age in any group, our data suggest that iron accumulation over time in the episodic migraine and CDH groups may be caused by repeated headaches. The intercept values of the correlation analyses in both migraine groups also support the possibility that tissue iron values were higher than normal at the outset in migraine-susceptible individuals, suggesting that high iron in the PAG may be fundamental to the cause of migraine.

Decreased R2' and R2* of RN and SN were recorded in the CDH patient group, best explained by activation and hyperoxia of these structures caused by headache during the study. Activation of the RN and SN was observed previously using fMRI-BOLD [5]; the precise reasons remain to be established but include both nociceptive and autonomic dysfunction. The PAG showed no evidence of similar activation to the RN and SN in the CDH group, possibly because of dysfunction or because high tissue non-heme iron may have attenuat-

ed changes in fMRI-BOLD signal. Such attenuation plus less flow activation during the mild to moderate headache of CDH may explain the absence of activation in contrast to the PET studies during an acute migraine episode [13].

As noted previously, the concentration of transferrin receptors that transport iron in and out of the PAG is the highest of any brain region [2]. Morphine injected into the PAG down-regulates transferrin receptors, indicating that PAG iron content also may be influenced by nociceptive activity [16]. Transferrin receptor density may be a marker of the cellular requirements for iron during oxidative metabolism [3]. High tissue iron levels may suggest that the PAG is abnormally metabolically active in migraine, even between episodic migraine attacks, or has a higher density of metabolically active neurons. These may be the factors that explain a high PAG iron early in migraine history, inferred from the high intercept values found in both patient groups. This did not explain the accumulation of iron over time, however. Irrespective, this emphasizes functional differences in the PAG in migraine subjects compared to normals.

Accumulation of iron in the PAG with the increasing burden of attacks and duration of illness may be explained by iron-catalyzed free radical cell damage, accentuated by repeated episodes of hyperoxia during migraine attacks [5, 6]. PAG iron levels were equally abnormally high in the episodic migraine and CDH patients. Our original concept was that iron accumulation would be a marker of progressive PAG dysfunction and responsible for evolution of episodic to chronic head pain, i.e. transformed migraine. No differences were found between the EM and CDH groups with respect to levels of tissue iron and its accumulation with the duration of illness to support this hypothesis. In the CDH group, however, the episodic migraine stage before the beginning of daily headache was not associated with iron increase, but the total duration of illness was strongly associated. This suggests a critical threshold in time for iron accumulation before CDH develops. Either this gives rise to more frequent triggering of migraine headache or PAG dysfunction could enhance the susceptibility of migraine patients to develop drug-induced rebound or chronic daily headache [17]. This is compatible with the concept of withdrawal excitation of the PAG associated with opioid addiction and its behavioral consequences [18].

Increased PAG iron levels were common to migraine with or without aura. Currently conceived as due to spreading depression triggered in hyperexcitable occipital cortex

[6], migraine aura is difficult to explain on the basis of PAG dysfunction. Nevertheless, experimental PAG stimulation produces widespread increase in cortical blood flow that is NO-mediated [19]. Also, the dorsal raphe component of the PAG sends diffuse serotonergic projections to the cerebral cortex and vessels that could influence neuronal excitability and vasomotor control [20]. It remains to be determined if these ascending projections contribute to hyperexcitability or in some way alter the threshold for triggering migraine aura.

Directly implicating PAG dysfunction as a cause of headache through interruption of its normal anti-nociceptive function seems plausible. During attacks of migraine without aura, Weiller et al. [13] observed consistent increases in regional cerebral blood flow in brainstem regions that covered PAG, midbrain reticular formation and the locus ceruleus. Activation continued despite alleviation of headache with treatment. Accordingly, the authors postulated that these centers were "generators" of migraine headache. However, the PAG is at the center of a major nociceptive system so that activation should be associated with alleviation of headache, particularly by gating the ascending flow of pain impulses to the thalamus [21]. Although the functions of the PAG are complex, presumably, a dysfunctional PAG is unable to switch-on effective nociception in the trigemino-vascular system when a migraine attack is triggered. This calls into question the concept of the PAG as an active generator of migraine, unless there are regions of PAG that activate pain because of aberrant function. In this regard, PAG dysfunction might alter the balance of descending influence of "on/off" neurons on pain transmission, enhancing the "on" pain-facilitating network [1].

Finally, epidemiological evidence for decreased prevalence of migraine attacks in the majority of older subjects may argue against permanent structural change in the PAG [22], and accordingly against its critical role in migraine. But shifts in factors that govern the threshold for migraine attacks may be extrinsic to PAG dysfunction, such as estrogen fluctuations or altered responsiveness of the neurovascular networks that activate migraine or are activated during migraine [23]. Again, this supports the existence of triggers of migraine lying outside the domain of the PAG, as well as a dysfunctional PAG that cannot respond effectively by switching on pain suppression.

References

1. Fields HL, Basbaum AI (1994) Central nervous system mechanisms of pain modulation. In: Wall PD, Melzack R (eds) Textbook of pain. Churchill Livingstone, Edinburgh, pp 243–257

2. Morris CM, Candy JM, Omar S, Bloxham CA, Edwardson JA (1994) Transferrin receptors in the parkinsonian midbrain. Neuropathol Appl Neurobiol 20(5):468–472

3. Morris CM, Candy JM, Bloxham CA, Edwardson JA (1993) Distribution of transferrin receptors in relation to cytochrome oxidase activity in the human spinal cord, lower brainstem and cerebellum. Adv Exp Med Biol 331:129–136

4. Adams JD Jr, Odunze IN (1991) Oxygen free radicals and Parkinson's disease. Free Rad Biol Med 10:161–169

5. Welch KMA, Cao Y, Aurora SK, Wiggins G, Vikingstad EM (1998) MRI of the occipital cortex, red nucleus, and substantia nigra during visual aura of migraine. Neurology 51:1465–1469

6. Cao Y, Welch KMA, Aurora S, Vikingstad EM (1999) Functional MRI-BOLD of visually triggered headache in patients with migraine. Arch Neurol 56(5):548–554

7. Gelman N, Gorell JM, Barker PB, Savage RM, Spickler EM, Windham JP, Knight RA (1999) MR Imaging of human brain at 3.0 T: preliminary report of transverse relaxation rates and relation to estimated iron content. Radiology 210:759–767

8. – (1988) Classification and diagnostic criteria for headache disorders, cranial neuralgias and facial pain. Classification Committee of the International Headache Society. Cephalalgia 8:1–96

9. Ma J, Wehrli FE (1996) Method for image-based measurement of the reversible and irreversible contribution to the transverse relaxation rate. J Magn Reson B 111:61–69

10. Bezdek JC (1980) A convergence theorem for the fuzzy ISODATA clustering algorithm. IEEE Trans Pattern Anal Mach Intell PAMI-2 1:1–8

11. Raskin NH, Hosobuchi Y, Lamb S (1987) Headache may arise from perturbation of brain. Headache 27:416–420

12. Haas DC, Kent PF, Friedman DI (1993) Headache caused by a single lesion of multiple sclerosis in the periaqueductal gray area. Headache 33:452–455

13. Weiller C, May A, Limmroth V, Juptner M, Kaube H, Schayk RV, Coenen HH, Diener HC (1995) Brainstem activation in spontaneous human migraine attacks. Nat Med 1:658–660

14. Smith GS, Savery D, Marden C, Lopez Costa JJ, Averill S, Priestley JV, Rattray M (1994) Distribution of messenger RNAs encoding enkephalin, substance P, somatostatin, galanin, vasoactive intestinal polypeptide, neuropeptide Y, and calcitonin gene-related peptide in the midbrain periaqueductal grey in the rat. J Comp Neurol 350(1):23–40

15. Bandler R, Carrive P (1988) Integrated defence reaction elicited by excitatory amino acid microinjection in the midbrain periaqueductal grey matter region of the unrestrained cat. Brain Res 439:95–106

16. Gomez-Flores R, Weber RJ (1999) Inhibition of interleukin-2 production and downregulation of IL-2 and transferrin receptors on rat splenic lymphocytes following PAG morphine administration: a role in natural killer and T cell suppression. J Interferon Cytokine Res 19(6):625–630

17. Christie MJ, Williams JT, Osborne PB, Bellchambers CE (1997) Where is the locus in opioid withdrawal? Trends Pharmacol Sci 18:13–140

18. Chieng B, Keay KA, Christie MJ (1995) Increased fos-like immunoreactivity in the periaqueductal gray of anaesthetised rats during opiate withdrawal. Neurosci Lett 183(1):37–40

19. Nakai M, Maeda M (1996) Nitrergic cerebral vasodilation provoked by the periaqueductal grey. Neuroreport 7:2571–2574

20. Cohen Z, Ehret M, Maitre M, Hamel E (1995) Ultrastructural analysis of tryptophan hydroxylase immunoreactive nerve terminals in the rat cerebral cortx and hippocampus: Their association with local blood vessels. Neuroscience 66:555–569

21. Goadsby PJ, Fields HL (1998) On the functional anatomy of migraine. Ann Neurol 43(2):272

22. Stewart WF, Lipton RB, Celentano DD, Reed ML (1992) Prevalence of migraine headache in the United States. JAMA 267:64–69

23. Welch KMA, Darnley D, Simkins RT (1984) The role of estrogen in migraine: a review and hypothesis. Cephalalgia 4(4):227–236